



Analysis for nonradiative recombination loss and radiation degradation of Si space solar cells

Masafumi Yamaguchi¹ | Kan-Hua Lee¹ | Kenji Araki¹ | Nobuaki Kojima¹ |
Yasuki Okuno² | Mitsuru Imaizumi³

¹Semiconductors Laboratory, Toyota Technological Institute, 2-12-1 Hisakata, Tempaku, Nagoya, 468-8511, Japan

²Institute for Materials Research, Tohoku University, 2-1-1 Katahira, Aoba-ku, Sendai, 980-8577, Japan

³Research and Development Directorate, Japan Aerospace Exploration Agency, 2-1-1 Sengen, Tsukuba, Ibaraki, 305-8505, Japan

Correspondence

Masafumi Yamaguchi, Toyota Technological Institute, 2-12-1 Hisakata, Tempaku, Nagoya 468-851, Japan.

Email: masafumi@toyota-ti.ac.jp

Abstract

Silicon space solar cells are currently attracting attention again for their relatively low-cost feature with sufficient performance, and they are expected to resume into the space market especially by short-term mission spacecraft designers. In this paper, efficiency potential of crystalline Si space solar cells is analyzed by considering external radiative efficiency (ERE), voltage and fill factor losses. Crystalline Si space solar cells have efficiency potential of more than 26% by realizing ERE of 20% from about 0.2% and normalized resistance of less than 0.05 from around 0.15. Nonradiative recombination and resistance losses in Si space solar cells are also discussed. Radiation degradation of Si space solar cells is also analyzed. Advanced Si solar cells such as passivated emitter, hetero-junction, and back contact solar cells are expected to use as space solar cells. Potential of advanced Si solar cells for space applications is discussed from point view of radiation degradation.

KEY WORDS

crystalline Si space solar cells, nonradiative recombination loss, radiation degradation, resistance loss

1 | INTRODUCTION

The silicon space solar cells^{1–3} have contributed to communications, broadcasting, weather forecasting, and scientific developments since the Vanguard-1 launched in 1958. Because space solar cells operate under severe conditions such as vacuum, high fluence high energy electron and proton irradiations and thermal cycle conditions, development of superior radiation resistant, and highly reliable space cell are necessary as well as high efficiency and low cost. Figure 1 shows chronological improvements in AM0 beginning-of-life (BOL) and end-of-life (EOL) efficiencies^{1–4} of Si space solar cells in comparison with AM1.5G efficiencies of crystalline Si solar cells for terrestrial use^{5–9} and future efficiency predictions of various Si solar cells (original idea by Professor A. Goetzberger¹⁰ and modified by M. Yamaguchi¹¹). The function chosen here (Equation 1) is derived from the diode equation:

$$\eta(t) = \eta_L \{1 - \exp[(a_0 - a)/c]\}, \quad (1)$$

where $\eta(t)$ is the time-dependent efficiency, η_L limiting asymptotic maximum efficiency, a_0 is the year for which $\eta(t)$ is zero, a is the calendar year, and c is a characteristic development time. For example, 29% for η_L , 30 for a_0 , and 1948 for c were used in the case of crystalline Si solar cells for terrestrial use. The function can be fitted relatively well to the past development of best laboratory efficiencies of crystalline Si cells. In Figure 1, equivalent AM0 efficiencies estimated for Si terrestrial solar cells were also plotted. The estimation procedure is presented in Section 2. The space solar cells are evaluated under AM0 illumination of 136.6 mW/cm², although the terrestrial solar cells are evaluated under AM1.5G illumination of 100 mW/cm². Therefore, efficiency ratio of AM0/AM1.5G for various solar cells is thought to be about 0.9 as shown in Figure 2.

As shown in Figure 1, high-efficiency crystalline Si solar cells with efficiencies of greater than 25% have been developed by using advanced technologies such as hetero-junction, back contact, and

passivated structures^{5–9} although those are for terrestrial use recently. Although 20.8% AM0 efficiency has been demonstrated with Passivated Emitter and Rear Locally diffused (PERL) solar cell,⁴ their radiation-resistance shown was lower compared with conventional Si space solar cells.

As also indicated in Figure 1, development of space silicon solar cell has been terminated in 1990's. This is because InGaP/GaAs/Ge structure high-efficiency triple-junction space solar cells were developed and introduced in the space market. The triple-junction cells also have better radiation resistance. However, triple-junction solar cells are essentially high-cost. Thus, silicon solar cells are currently attracting attention again for their relatively low-cost feature with suf-

ficient performance, and they are expected to resume into the space market especially by short-term mission spacecraft designers.

Therefore, clarifying nonradiative recombination loss, resistance loss, and radiation resistance in current Si space solar cells and advanced Si solar cells for terrestrial use is very important for further development of high-performance Si space solar cells. This paper presents analytical results for nonradiative recombination loss, resistance loss, and radiation resistance of current crystalline Si space solar cells and advance Si solar cells for terrestrial use.

2 | ANALYSIS FOR EFFICIENCY POTENTIAL OF CRYSTALLINE SI SPACE SOLAR CELLS

In this section, current status of efficiencies of crystalline Si space solar cells and advanced Si solar cells for space use is analyzed by using external radiative efficiency (ERE) and voltage and fill factor losses.

One of problems to attain the higher efficiency crystalline Si solar cells is the longer minority-carrier lifetime in Si. Radiative recombination lifetime τ_{rad} is expressed by

$$\tau_{rad} = 1/BN, \quad (2)$$

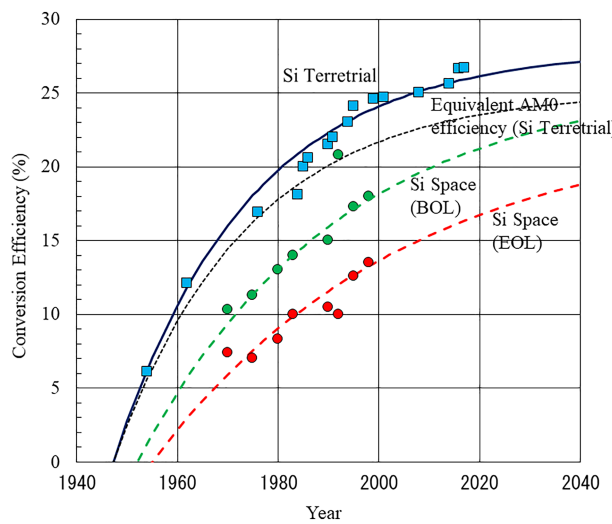


FIGURE 1 (Color online) Chronological improvements in AM0 beginning-of-life (BOL) and end-of-life (EOL) efficiencies^{1–4} of Si space solar cells in comparison with AM1.5G efficiencies of crystalline Si solar cells for terrestrial use^{5–9} and future efficiency predictions of various Si solar cells (original idea by Professor A. Goetzberger¹⁰ and modified by Yamaguchi¹¹) [Colour figure can be viewed at wileyonlinelibrary.com]

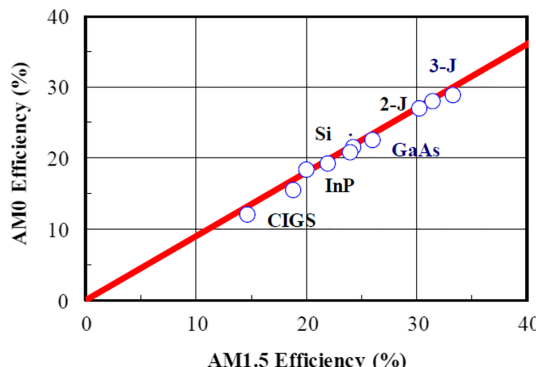


FIGURE 2 (Color online) Correlation between AM0 and AM1.5G characteristics of various solar cells made for terrestrial use

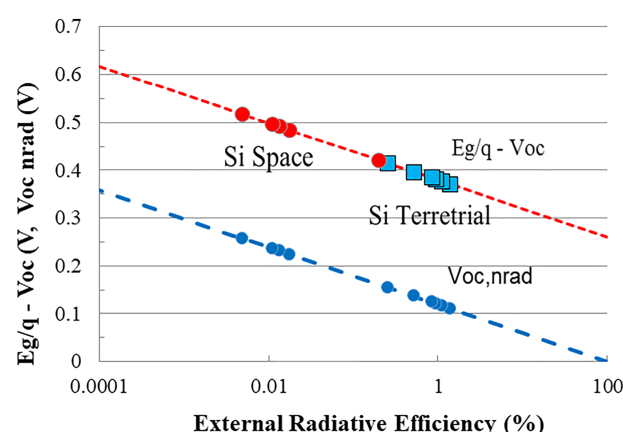


FIGURE 3 (Color online) Open-circuit voltage drop compared to bandgap energy ($E_g/q - V_{oc}$) and nonradiative V_{oc} ($V_{oc, nrad}$) in Si solar cells as a function of external radiative efficiency (ERE). Circles and squares for $E_g/q - V_{oc}$ data show data for Si space cells^{1–4} and data^{5–9} for advanced cells for terrestrial use, respectively

where τ_{nonrad} is nonradiative recombination lifetime, where σ is capture cross section of minority-carriers by nonradiative recombination centers, v is minority-carrier thermal velocity, and N_r is density of nonradiative recombination center. Therefore, improvements in Si crystalline quality and reduction in densities of defects such as dislocations, grain boundaries, and impurities that act as nonradiative recombination centers are very important.

In order to realize higher efficiency of various solar cells, improvements in short-circuit density J_{sc} , open-circuit voltage V_{oc} , and fill factor FF are substantially necessary.

The open-circuit voltage V_{oc} is given by

$$V_{oc} = \frac{kT}{q} \ln \left(\frac{J_L}{J_0} + 1 \right), \quad (4)$$

where k is Boltzmann constant, T is absolute temperature, q is electronic charge, J_L is photon generated current density, and J_0 is saturation current density. In order to increase V_{oc} , decrease in saturation current density J_0 is essential.

One of problems to attain the higher efficiency solar cells is the higher minority-carrier lifetime in various materials and thus reduction in voltage loss. Figure 3 shows open-circuit voltage drop compared to bandgap energy ($E_g/q \cdot V_{oc}$) and nonradiative voltage loss ($V_{oc,rad}$) in Si solar cells as a function of ERE.^{13–17} Open-circuit voltage is expressed by^{13–17}

$$V_{oc} = V_{oc,rad} + \frac{kT}{q} \ln(EPE), \quad (5)$$

where the second term shows nonradiative voltage loss, and $V_{oc,rad}$ is radiative open-circuit voltage and is given by^{13–17}

$$V_{oc,rad} = \frac{kT}{q} \ln \left(\frac{J_L(V_{oc,rad})}{J_{0,rad}} + 1 \right), \quad (6)$$

where $J_L(V_{oc,rad})$ is photo-induced current density at open-circuit in the case of only radiative recombination and $J_{0,rad}$ is the saturation current density in the case of only radiative recombination and 0.86 V was used as the $V_{oc,rad}$ value¹⁷ in this study. Determination procedure of radiative open-circuit voltage is shown in the reference.¹⁸

In Figure 3, V_{oc} values for PERL cell,^{5,9} Heterojunction with Intrinsic Thin-layer (HIT) cell,⁶ Back-contact cell,⁹ Hetero-junction Back Contact (HBC) cell,^{7–9} and Si space solar cells.^{1–4} Si solar cells and ERE values in the references and values estimated by using Equations 5 and 6 are plotted. As shown in Figure 3, compared with high-efficiency crystalline Si solar cells for terrestrial use, Si space solar cells have higher nonradiative recombination loss and further improvements in efficiency are thought to be possible by improving minority-carrier lifetime and reducing nonradiative recombination and resistance losses. In order to improve the V_{oc} , increasing ERE shown in Equation 5 is necessary. That is, reduction in nonradiative voltage loss is necessary. One of the most important issues for improving the V_{oc} is to reduce nonradiative recombination loss and thus to increase

minority-carrier lifetime in solar cells because the nonradiative open-circuit voltage is given by the following equation

$$V_{oc,rad} = \frac{kT}{q} \ln \left[\frac{\tau_{nonrad}}{\tau_{rad} + \tau_{nonrad}} \right]. \quad (7)$$

Therefore, efficiency potential of crystalline Si space solar cells is analyzed by considering nonradiative recombination loss and minority-carrier lifetime in this study.

Figure 4 shows calculated AM0 efficiencies of crystalline Si space solar cells as a function of ERE in comparison with state-of-the-art efficiencies of Si space solar cells^{1–3} and AM0 efficiencies of PERL cells.⁴ Limiting efficiencies of crystalline Si solar cells for terrestrial use reported are 28.4% by Swanson,¹⁹ 29.4% by Ritcher et al.,²⁰ and 28.5% by the authors.¹⁴ As shown in Figure 4, Si space solar cells have efficiency potential of more than 26% by realizing ERE of 20% from about 0.2% and normalized resistance of less than 0.05 from around 0.1. Although 26.7% efficiency ($J_{sc} = 42.65 \text{ mA/cm}^2$, $V_{oc} = 0.738 \text{ V}$, $FF = 0.849$) under AM1.5G illumination has been demonstrated with Si HBC solar cells,⁸ 20.8% efficiency ($J_{sc} = 50.5 \text{ mA/cm}^2$, $V_{oc} = 0.701 \text{ V}$, $FF = 0.805$) under AM0 illumination has been attained with Si PERL solar cells.⁴ The parameters for Si solar cells with limiting efficiency of 29.43%²⁰ under AM1.5G illumination are $J_{sc} = 43.31 \text{ mA/cm}^2$, $V_{oc} = 0.7613 \text{ V}$, and $FF = 0.8926$. Those for Si solar cells with possible efficiency of 26% under AM0 illumination $J_{sc} = 53.0 \text{ mA/cm}^2$, $V_{oc} = 0.800 \text{ V}$, and $FF = 0.843$. Compared with limiting AM0 efficiency of about 26%, there are still large gap for current Si space solar cells.

Fill factor is dependent upon V_{oc} and ideal fill factor FF_0 used in the calculation is empirically expressed by,²¹

$$FF_0 = \frac{V_{oc} - \ln(V_{oc} + 0.72)}{V_{oc} + 1}, \quad (8)$$

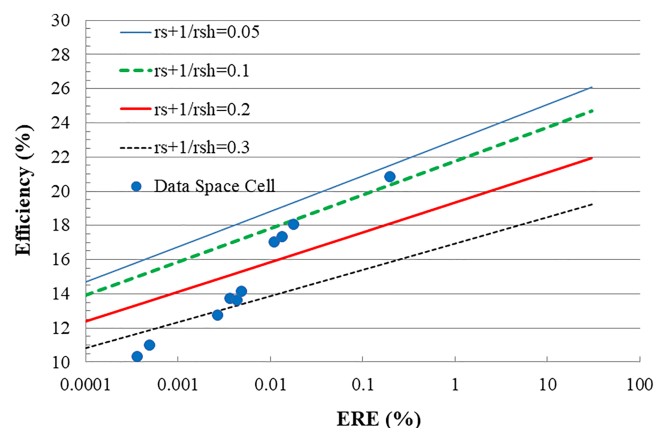


FIGURE 4 (Color online) Calculated AM0 efficiencies of crystalline Si space solar cells as a function of external radiative efficiency (ERE) in comparison with state-of-the-art efficiencies of Si space solar cells^{1–3} and AM0 efficiencies of Passivated Emitter and Rear Locally diffused (PERL) cells⁴

where v_{oc} is normalized open-circuit voltage and is given by

$$v_{oc} = V_{oc}/(nkT/q). \quad (9)$$

The fill factor is decreased as increase in series resistance R_s and decrease in shunt resistance R_{sh} of solar cell increases and expressed by²¹

$$FF = FF_0(1 - r_s)(1 - 1/r_{sh}), \quad (10)$$

where r_s is normalized series resistance and r_{sh} is normalized shunt resistance and are given by²¹

$$r_s = R_s/R_{CH}, \quad (11)$$

$$r_{sh} = R_{CH}/R_{sh}. \quad (12)$$

The characteristic resistance R_{CH} is expressed by²¹

$$R_{CH} = \frac{V_{oc}}{I_{sc}}. \quad (13)$$

In the analysis, nonradiative voltage loss as expressed by the following equation was estimated and nonradiative recombination lifetime τ_{nonrad} was estimated by using Equations 2, 3, 5, and 14.

$$V_{oc,nonrad} = \frac{kT}{q} \ln[\tau_{nonrad}/(\tau_{rad} + \tau_{nonrad})]. \quad (14)$$

V_{oc} was estimated by using Equations 2, 3, 5, and 14, and FF was estimated by using Equation 5 and from Equations 7 to 14. In the calculation, 53 mA/cm² under AM0 was used as J_{sc} by estimating ideal J_{sc} from standard AM0 spectrum.²² V_{oc} value under AM0 illumination is slightly higher than that under AM1.5G illumination because V_{oc} is expressed by Equation 4, and J_{sc} value under AM0 illumination is higher than that under AM1.5G illumination.

Figure 5 shows chronological improvement of (a) ERE and (b) resistance loss ($1 - 1/r_s - 1/r_{sh}$) analyzed for Si space solar cells.^{1–4} As shown in Figure 5, ERE values were improved with back surface field (BSF), back surface reflector (BSR), back surface field and reflector (BSFR), and nonreflective surface structures from conventional

n-on-p type homo junction solar cells as a result of J_{sc} increase due to improvements in long wavelength response and short wavelength response, and V_{oc} increase due to decrease in dark current density. Resistance losses were also improved as a result of improvements grid figure patterning and cell processing and thinning of Si space solar cells.

3 | ANALYSIS OF RADIATION RESISTANCE OF CURRENT CRYSTALLINE SI SPACE SOLAR CELLS

Although effectiveness of p-type base and thinner cell from the point-of-view radiation-resistance has been shown by several references,^{1–3} radiation-resistance and efficiency potential of various Si space solar cells is presented by using analytical procedure developed by the authors in order to clarify effectiveness of advanced Si solar cells compared with in this section.

3.1 | Improvements in radiation-resistance of Si space solar cells by improving device structures

As shown in Figure 6, ERE values were improved with BSF, BSR, BSFR, and nonreflective surface structures from conventional n-on-p type homo junction solar cells^{1–3} as a result of J_{sc} increase due to improvements in long wavelength response and short wavelength response, and V_{oc} increase due to decrease in dark current density. Resistance losses were also improved as a result of improvements grid figure patterning and cell processing and thinning of Si space solar cells.

Figure 6 shows changes in (a) output power and (b) remaining factor of output power of Si space solar cells with various structures as a function of 1 MeV electron fluence.^{1–3} Although output power of Si space solar cells has been improved by improving device structures from conventional homo-junction cell structures to BSF, BSR, BSFR, and nonreflecting surface structures (NRS) as shown in Figure 6a, remaining factor of output power of Si space solar cells with higher efficiency is slightly lower as shown in Figure 6b. In general, the poorer efficiency solar cells show relatively the higher radiation resistance in the case that radiation degradation of solar cells is limited by minority-carrier lifetime (diffusion length) as expressed by the following equation. Recombination centers tend to affect the solar cell

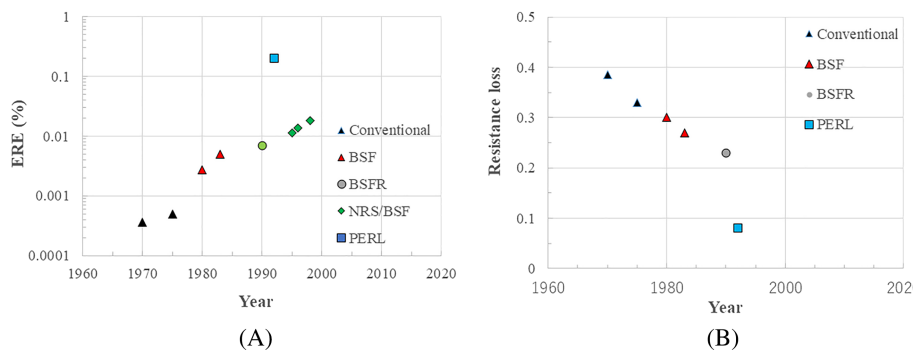


FIGURE 5 (Color online)
Chronological improvement of
(a) external radiative efficiency (ERE) and
(b) resistance loss ($1 - 1/r_s - 1/r_{sh}$)
analyzed for Si space solar cells^{1–4}

FIGURE 6 (Color online) Changes in (a) output power and (b) remaining factor of Si space solar cells with various structures as a function of 1 MeV electron fluence^{1–3}

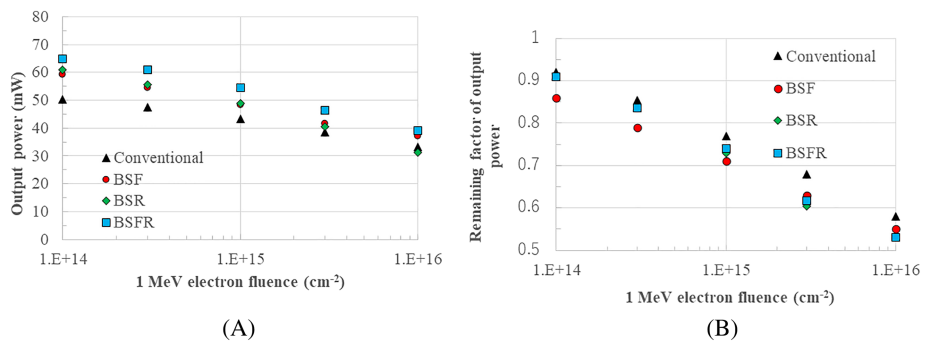


FIGURE 7 (Color online) Changes in (a) output power and (b) remaining factor of Si space solar cells with base carrier concentration (resistivity) as a function of 1 MeV electron fluence^{1–3}

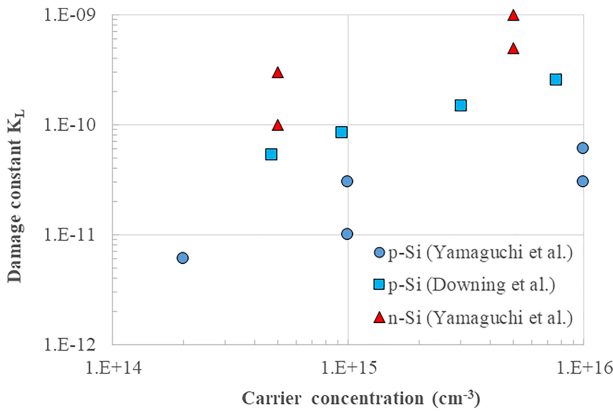
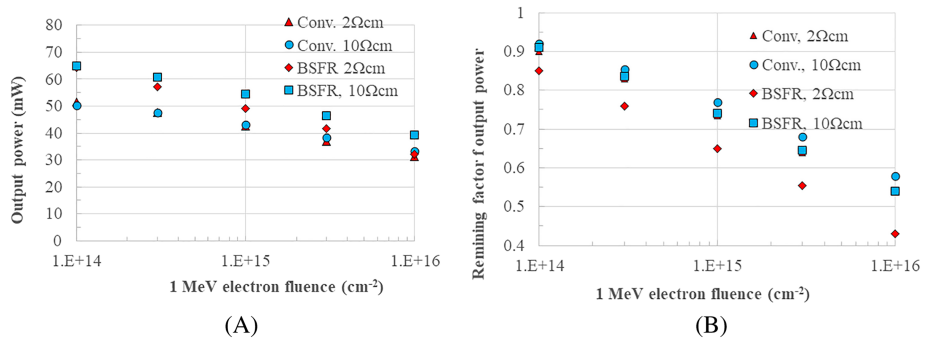


FIGURE 8 (Color online) Changes in damage constant for minority-carrier diffusion length as a function of carrier concentration in p-type Si and n-type Si reported by the authors^{23,24} and Downing et al.²⁵

performance by reducing the minority carrier diffusion length of electrons in the p-type base, L , (or equivalently lifetime, τ , using $L = (D\tau)^{1/2}$) from a preirradiation value L_0 to a postirradiation value L_φ through equation

$$\frac{1}{L_\varphi^2} - \frac{1}{L_0^2} = \sum I_{ri} \sigma_i v_{th} \varphi / D = K_L \varphi, \quad (15)$$

where suffixes 0 and φ show before and after irradiation, respectively, I_{ri} is introduction rate of i th recombination center by electron irradiation, σ_i the capture cross section of minority-carrier by i th recombination center, v_{th} the thermal velocity of minority-carrier, D the minority-carrier diffusion coefficient, K_L the damage coefficient for minority-carrier diffusion length, and φ the electron fluence.

In addition, effects of BSF and BSR are thought to be decreased after high-fluence irradiation.

3.2 | Effects of carrier concentration (resistivity) of base-layer on radiation-resistance of Si space solar cells

Figure 7 shows changes in (a) output power and (b) remaining factor of output power of Si space solar cells with base carrier concentration (resistivity) as a function of 1 MeV electron fluence.^{1–3} Although differences in BOL efficiency of Si space solar cells with various base resistivity are thought to be quite smaller as shown in Figure 7a, it is clear that radiation-resistance of Si space solar cells with higher resistivity (lower carrier concentration) base shows the higher radiation-resistance compared with that of Si space cells with lower resistivity (higher carrier concentration) as shown in Figure 7b.

Effects of base resistivity (carrier concentration) on radiation-resistance of Si space solar cells are explained by carrier concentration dependence of damage constant for minority-carrier diffusion length as expressed by Equation 15. Figure 8 shows changes in damage constant for minority-carrier diffusion length as a function of carrier concentration in p-type Si and n-type Si reported by the authors^{23,24} and Downing et al.²⁵ Because major radiation-induced defects are known to be di-vacancy (V-V) defect, carbon interstitial (C_i)-oxygen interstitial (O_i) complex defect, and boron interstitial (B_i)-oxygen interstitial (O_i) complex defects^{26,27} in the case of p-type Si, damage constant for minority-carrier diffusion length is shown to be dependent on carrier concentration due to boron-related defects. Effects of damage

constant on radiation degradation of Si solar cells are further discussed in Sections 4.2 and 5.

3.3 | Effects of cell thickness on radiation-resistance of Si space solar cells

Thinning solar cells are thought to be effective for improvements in radiation-resistance of Si space solar cells. Figure 9 shows changes in (a) output power and (b) remaining factor of output power of Si space solar cells with various thickness as a function of 1 MeV electron fluence.^{1–3} Even in thin Si space solar cells, output power of Si space solar cells has been improved by improvements in device fabrication

technologies, carrier confinement and light trapping as shown in Figure 9a. In addition, it is clear that remaining factor of output power of Si space solar cells with the thinner is higher compared with thicker cells as shown in Figure 9b. Thinner Si space solar cells are expected as superior radiation-resistant, light-weight, and low-cost space cells.

4 | ANALYSIS OF RADIATION DEGRADATION OF ADVANCED SI SOLAR CELLS

Advanced solar cells such as PERL solar cells,⁵ hetero-junction solar cells⁶ and back contact solar cells^{28,29} are expected as Si space solar

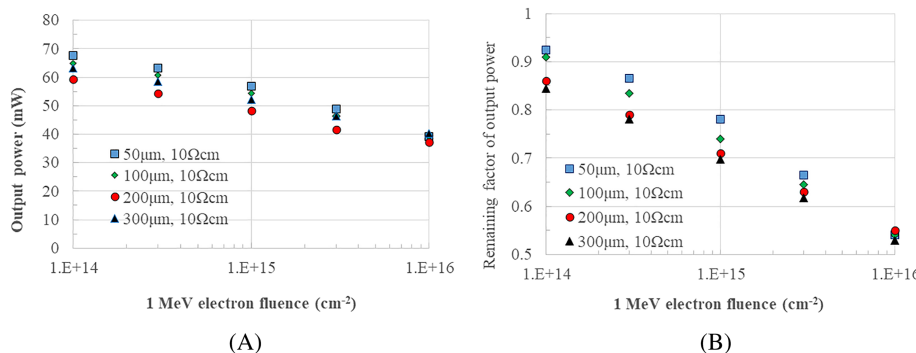


FIGURE 9 (Color online) Changes in (a) output power and (b) remaining factor of Si space solar cells with various thickness as a function of 1 MeV electron fluence^{1–3}

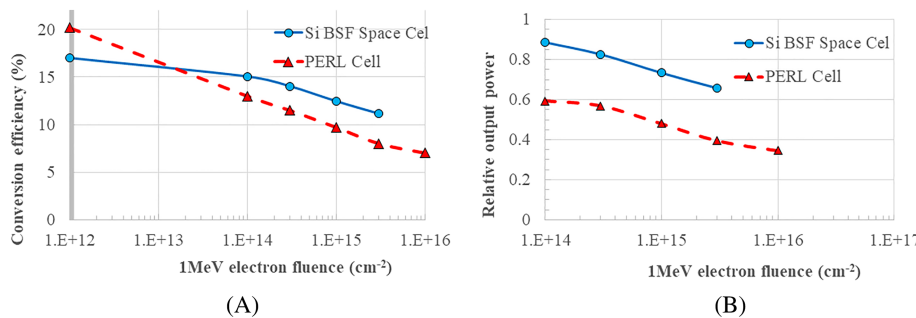


FIGURE 10 (Color online) Changes in (a) conversion efficiency and (b) remaining factor of output power of Si Passivated Emitter and Rear Locally diffused (PERL) solar cells⁴ as a function of 1 MeV electron fluence

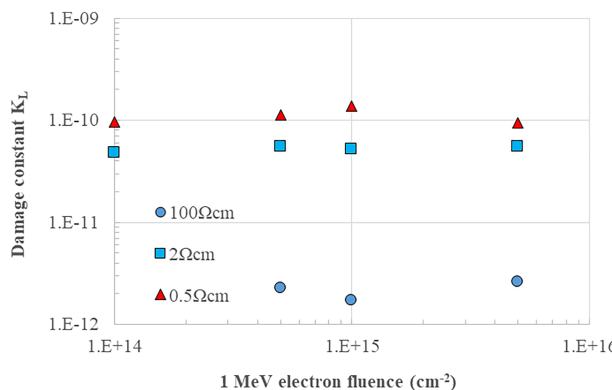


FIGURE 11 (Color online) Changes in damage constant for minority-carrier diffusion length estimated by using Equation 15 in Si Passivated Emitter and Rear Locally diffused (PERL) solar cells⁴ as a function of 1 MeV electron fluence

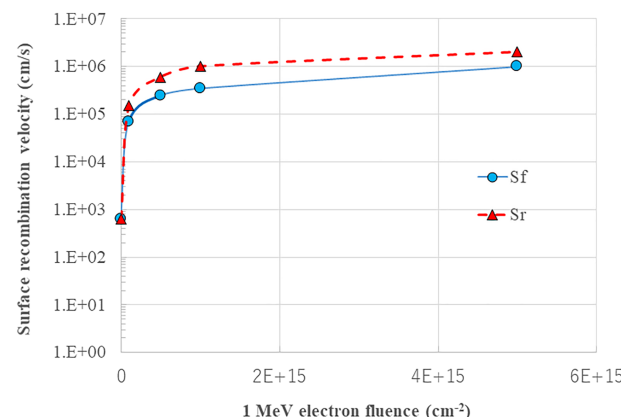


FIGURE 12 (Color online) Changes in front and rear surface recombination velocity of Si Passivated Emitter and Rear Locally diffused (PERL) solar cells⁴ due to 1 MeV electron irradiations

cells because of high-efficiency potential. In this section, radiation degradation of advance Si solar cells is analyzed.

4.1 | Analysis for radiation degradation of passivated structure Si solar cells

Figure 10 shows changes in (a) conversion efficiency and (b) remaining factor of output power of Si PERL solar cells⁴ as a function of 1 MeV electron fluence. Although BOL efficiency of PERL solar cells is higher than that of Si BSFR space solar cells, radiation degradation of PERL solar cells is severe compared to Si BSFR space solar cells. Figure 11 shows changes in damage constant for minority-carrier diffusion length estimated by using Equation 15 in Si PERL solar cells⁴ as a function of 1 MeV electron fluence. As shown in Figure 11, damage constant for minority-carrier diffusion length in Si PERL solar cells⁴ is the similar with that in current Si space solar cells,²² although radiation degradation of Si solar cells is dependent on resistivity of Si wafer (base-layer) as shown in Figure 7. There must be the other mechanism on radiation degradation of Si PERL solar cells.

Figure 12 shows changes in front and rear surface recombination velocity S_f, S_r of Si PERL solar cells⁴ due to 1 MeV electron irradiations. According to Snow et al.,³⁰ building-up of a space charge within the oxide with ionizing radiation and creation of fast surface states at the oxide-Si interface are suggested to result in increasing surface recombination velocity. Therefore, poorer radiation-resistance of Si PERL cells compared to current Si space solar cells is thought to be attributed to increase in surface recombination in front and rear surfaces. In order to apply Si PERL solar cells into space use, to clarify mechanism on surface recombination degradation and to prevent from surface recombination velocity increase with irradiation is very important.

Formation of shallow junction depth from 0.7–1.5 μm to 0.1–0.15 μm in the similar with current Si space solar cells is thought

to be one of ideas to improve radiation-resistance of Si PERL solar cells. Effectiveness of shallow junction formation in the GaAs solar cells with high surface recombination velocity is well known.³¹ Figure 13 shows junction depth dependence of relative short-circuit current density of Si solar cells by considering degradation of surface recombination velocity and n-type emitter layer diffusion length in comparison with relative J_{sc} degradation of Si PERL cells.⁴ The numerical analysis of properties of Si solar cells was performed using the device simulator PC1D ver. 5.9.^{32,33} Comparison between calculated and experimental results shown in Figure 13 suggests that another problem for Si space solar cells with deeper junction is higher degradation in n-type emitter layer. It is clear that the deeper junction Si solar cells are greatly degraded due to radiation degradation in emitter layer and surface recombination effects. As shown Figure 13, shallow junction formation is necessary in order to apply Si PERL cells into space use.

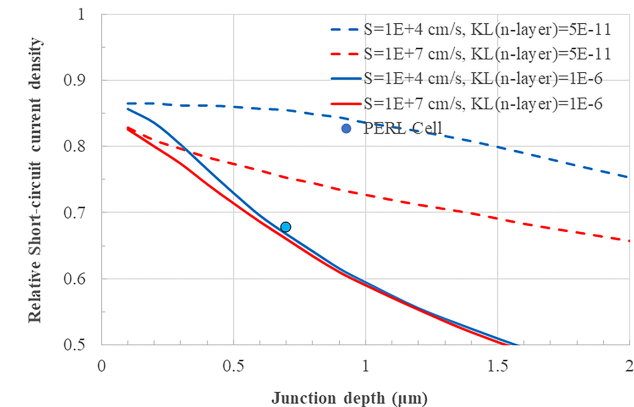
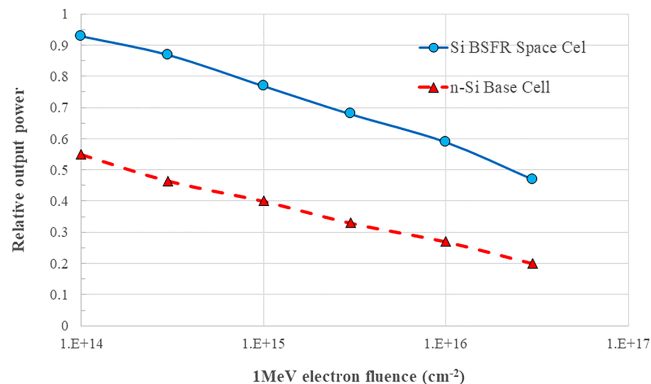


FIGURE 13 (Color online) Junction depth dependence of relative short-circuit current density of Si solar cells calculated by considering degradation of surface recombination velocity and n-layer diffusion length in comparison with relative J_{sc} degradation of Si Passivated Emitter and Rear Locally diffused (PERL) cells⁴

FIGURE 14 (Color online) Changes in relative output power of n-type Si base cells³⁴ as a function of 1 MeV electron fluence in comparison with those of Si back surface field and reflector (BSFR) space solar cells^{1–3}

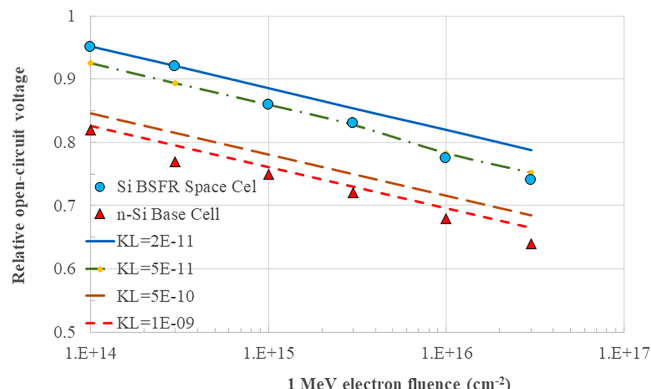


FIGURE 15 (Color online) Changes in relative output power of n-type Si base cells³⁴ as a function of 1 MeV electron fluence in comparison with those of Si back surface field and reflector (BSFR) space solar cells^{1–3} and calculated results for changes in relative output power of Si solar cells as a function of damage constant K_L for minority-carrier diffusion length

4.2 | Analysis for radiation degradation of high-efficiency Si solar cells with n-type Si base

The high-efficiency hetero-junction⁶ and back contact^{28,29} Si solar cells are thought to have also great potential of space applications but those solar cells are fabricated by using n-type Si base layer. Therefore, to clarify their radiation-tolerance of n-type Si is necessary.

Figure 14 shows changes in relative output power of n-type Si base cells³⁴ as a function of 1 MeV electron fluence in comparison with those of Si BSFR space solar cells.^{1–3} It is clear that n-type Si base solar cells show poorer radiation-resistance compared with p-type Si base solar cells.

Effects of conducting type on radiation-resistance of Si solar cells are explained by damage constant for minority-carrier diffusion length as expressed by Equation 15 as shown in Figure 8. Figure 15 shows changes in relative output power of n-type Si base cells³⁴ as a function of 1 MeV electron fluence in comparison with those of Si BSFR space solar cells^{1–3} and calculated results for changes in relative output power of Si solar cells as a function of damage constant K_L for minority-carrier diffusion length. Damage constant for minority-carrier diffusion length in n-type Si estimated from Figure 15 is 1×10^{-9} and is higher than (5×10^{-11}) in p-type Si. Major radiation-induced defects in n-type Si are thought to be di-vacancy (V-V), vacancy-oxygen (V-O) vacancy-phosphorous (V-P) complex defects, whereas those in p-type Si are well known to be di-vacancy (V-V), carbon interstitial (Ci)-oxygen interstitial (Oi), and boron interstitial (Bi)-oxygen interstitial (Oi) complex defects.^{26,27} Therefore, differences of damage constants for diffusion length in n-type Si and p-type Si are thought to be differences of introduction rated of recombination centers and capture cross sections for minority-carrier as expressed by Equation 15 in n-type Si and p-type Si.

4.3 | Analysis for radiation degradation of high-efficiency Si back contact solar cells

The high-efficiency back contact Si solar cells^{28,29} are thought to have also great potential of space applications. In this section, radiation degradation of Si back contact solar cells is analyzed by using results reported by Garboushian et al.³⁵ Figure 16 shows effects of cell thickness on relative output power of Si back contact solar cells³⁵ irradiated with $1 \times 10^{14} \text{ cm}^{-2}$ 1 MeV electrons in comparison with calculated results. It is clear that under even low-fluence irradiations of $1 \times 10^{14} \text{ cm}^{-2}$ 1 MeV electrons, Si back contact solar cells with thicker cell thickness are highly degraded.

In the case of Si back contact solar cells, short-circuit current density J_{sc} after irradiation is thought to be dependent on minority-carrier diffusion length L and wafer thickness d . Relative J_{sc} is expressed by

$$J_{sc\varphi}/J_{sc0} = \exp(-d/L_\varphi)/\exp(-d/L_0) \quad (16)$$

where subscripts 0 and φ are before and after irradiations. Figure 15 also shows analytical results calculated by using Equation 16. It is clear

that Si back contact solar cells with the thicker cells are degraded faster.

Figure 17 shows changes in relative output power of Si back contact solar cells³⁵ with various wafer thickness as a function of 1 MeV electron fluence in comparison with calculated results of Si back contact solar cells and experimental results for Si BSFR space solar cells. Even thin back contact solar cells with thickness of 50 μm shows poorer radiation-resistance compared with current Si space solar cells because decrease in J_{sc} by minority-carrier diffusion length degradation with irradiation in the back-side junction solar cells is more severe compared with front-side junction solar cells as shown in Equation 16. It is clear that Si back contact solar cells with the thicker cells are degraded faster and Si back contact solar cells are not thought to be appropriate for space use.

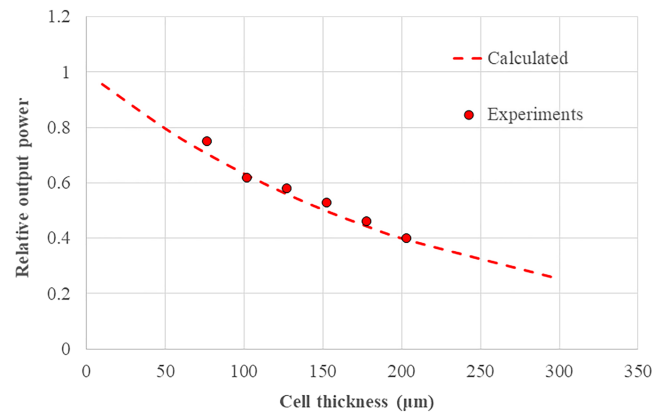


FIGURE 16 (Color online) Effects of cell thickness on relative output power of Si back contact solar cells³⁵ irradiated with $1 \times 10^{14} \text{ cm}^{-2}$ 1 MeV electrons in comparison with calculated results

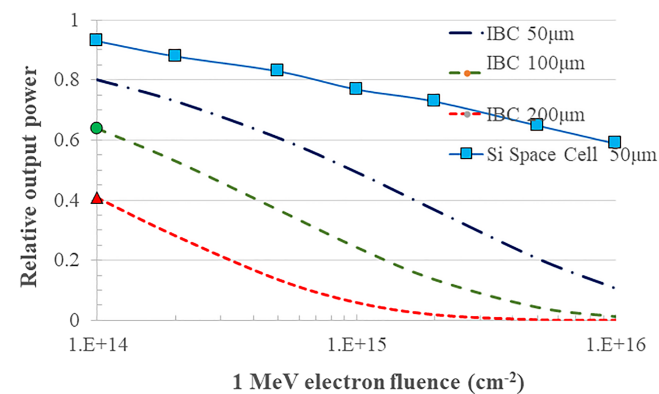


FIGURE 17 (Color online) Changes in relative output power of Si back contact solar cells with various wafer thickness as a function of 1 MeV electron fluence in comparison with calculated results of Si back contact solar cells³⁵ and experimental results for Si back surface field and reflector (BSFR) space solar cells^{1–3}

TABLE 1 Defect level activation energy E_a , introduction rate I_t and capture cross section σ of radiation-induced defects in p-type and n-type Si reported by the authors²⁶ and the others^{36–38}

	E_a (eV)	I_t (cm^{-1})	σ (cm^2)	Possible identification	References
p-Si (10 Ω cm, 1 MeV)	Ev + 0.18	0.003	8.9×10^{-17}	V-V	Yamaguchi et al. ²⁶
	Ev + 0.36	0.007	7.2×10^{-16}	C _i -O _i	Yamaguchi et al. ²⁶
	Ec – 0.18	0.013	1.8×10^{-16}	B _i -O _i	Yamaguchi et al. ²⁶
n-Si(100 Ω cm, 1 MeV)	Ec – 0.17	0.30			Carter ³⁶
	Ec – 0.4	0.025			Carter ³⁶
n-Si(100 Ω cm, 1.5 MeV)	Ec – 0.15		1×10^{-15}	V-O	Londos ³⁷
	Ec – 0.21		3.53×10^{-17}	V-V	Londos ³⁷
	Ec – 0.28		5.03×10^{-16}	V ₂ -O?	Londos ³⁷
	Ec – 0.33		8.8×10^{-17}	V ₂ -O ₂ ?	Londos ³⁷
	Ec – 0.45		1.1×10^{-16}	V-P	Londos ³⁷
n-Si(30 Ω cm, 6 MeV)	Ec – 0.165	0.12	7.5×10^{-15}	V-O	Markevich et al. ³⁸
	Ec – 0.24	0.025	2.5×10^{-15}	V-V	Markevich et al. ³⁸
	Ec – 0.425	0.025	1.1×10^{-15}	V-P	Markevich et al. ³⁸

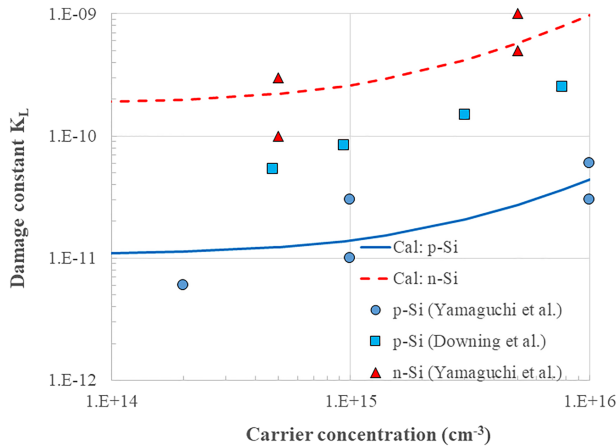


FIGURE 18 (Color online) Changes in damage constant for minority-carrier diffusion length as a function of carrier concentration in p-type Si and n-type Si reported by the authors^{23,24} and Downing et al.²⁵

defect level, introduction rate I_t and capture cross section for minority-carrier σ of radiation-induced defects in p-type Si and n-type Si reported by the authors²⁶ and the others.^{36–38}

Damage constant for minority-carrier diffusion length K_L calculated by using Equation 15 and data reported by the authors²⁶ and Markevich et al.³⁸ Regarding carrier concentration dependence of K_L , liner dependence of B and P concentration on introduction rates for B_i-O_i and V-P complex defects was assumed. Figure 18 shows changes in damage constant for minority-carrier diffusion length as a function of carrier concentration in p-type Si and n-type Si reported by the authors^{23,24} and Downing et al.²⁵ Because capture cross section for minority-carrier of V-P defect in n-type Si is higher than that of B_i-O_i in p-type Si as shown in Table 1, damage constant for minority-carrier diffusion length of n-type Si is higher compared with p-type Si as shown in Figure 8 and thus radiation degradation of n-type Si is higher compared with p-type Si as shown in Figures 14 and 15. Therefore, Si solar cells with n-type Si base is not thought to be useful for Si space solar cells and development of hetero-junction solar cells by using p-type Si base is necessary for space use.

5 | DISCUSSION ABOUT EFFECTS OF DEFECT INTRODUCTION RATE AND CAPTURE CROSS SECTION ON RADIATION DEGRADATION OF SI SOLAR CELLS

As shown in previous sections, defect degradation of Si space solar cells and advanced Si solar cells is sensitive to carrier concentration and conductive type. In this section, effects of introduction rate and capture cross section for minority-carrier of radiation-induced defects on radiation degradation of Si solar cells are discussed. As expressed by Equation 15, damage constant for diffusion length K_L is correlated to introduction rate I_t and capture cross section for minority-carrier σ of radiation-induced defects. Table 1 shows activation energy of

6 | SUMMARY

Silicon space solar cells are currently attracting attention again for their relatively low-cost feature with sufficient performance, and they are expected to resume into the space market especially by short-term mission spacecraft designers.

Efficiency potential of crystalline Si space solar cells is analyzed by analytical procedure developed by the authors. Crystalline Si space solar cells have efficiency potential of more than 26% by realizing ERE of 20% from about 0.2% and normalized resistance of less than 0.05 from around 0.15. Nonradiative recombination and resistance losses in Si space solar cells are also discussed. Radiation degradation of Si

space solar cells is also analyzed. Effects of base carrier concentration and cell thickness on radiation resistance of Si space solar cells are discussed.

Advanced Si solar cells such as passivated emitter, heterojunction and back contact solar cells are expected to use as space solar cells. Potential of advanced Si solar cells for space applications is discussed from the view point of radiation degradation. Because surface recombination velocity of the Si PERL solar cells are highly degraded, formation of shallower junction is suggested in order to improve their radiation resistance. The n-type Si base solar cells such as hetero-junction and back contact solar cells are found to be highly degraded compared with p-type Si base solar cells because damage constant for minority-carrier lifetime in n-type Si is higher than that in p-type Si. Development of p-type Si base hetero-junction solar cells is suggested for further improvement of performance for space applications, whereas the Si back contact solar cells are not thought to be radiation-resistant compared to normal front contact solar cells. This knowledge should lead to realization of improved space silicon solar cells which properties meet the demands in the recent space market.

ACKNOWLEDGMENTS

This work was based on discussions under JAXA's Research Committee for Radiation-Resistant Space Solar Cells. The authors would like to Committee members, Prof. Akio Ushirokawa and Prof. Michio Tajima, former Univ. Tokyo, Mr. Sumio Matsuda, former JAXA and Mr. Akio Suzuki and Mr. Tatsuo Saga, former Sharp Co., Dr. Steve J. Taylor, ESA, Prof. Aurangzeb Khan, Univ. South Alabama, and Prof. Koshi Ando, Tottori Univ. for their fruitful collaboration and cooperation.

ORCID

Masafumi Yamaguchi  <https://orcid.org/0000-0002-2825-7217>
 Kan-Hua Lee  <https://orcid.org/0000-0001-8560-1515>
 Kenji Araki  <https://orcid.org/0000-0002-3216-948X>
 Yasuki Okuno  <https://orcid.org/0000-0002-8569-4077>
 Mitsuru Imaizumi  <https://orcid.org/0000-0001-5456-1696>

REFERENCES

- Tada HY, Carter JR Jr, Anspaugh BE, Downing RG. Radiation Effects. *Solar Cell Radiation Handbook*. Third ed. Pasadena (NASA and JPL, USA): JPL PUBLICATION; 1982:3-1-3-152.
- Suzuki A. High-efficiency silicon space solar cells. *Sol Energy Mater Sol Cells*. 1998;50(1-4):289-303.
- Washio H, Katsu T, Tonomura Y, et al. Development high efficiency thin silicon space solar cells. *Proceedings of the 19th IEEE Photovoltaic Specialists Conference (IEEE, New York)*. 1993:p.1347-1351.
- Wang A. High efficiency PERC and PERL silicon solar cells. PhD Thesis. (UNSW, Sydney) 1992.
- Zhao J, Wang A, Green MA, Ferrazza F. Novel 19.8% efficient honeycomb textures multicrystalline and 24.4% monocrystalline silicon solar cells. *Appl Phys Lett*. 1998;73(14):1991-1993.
- Taguchi M, Yano A, Tohoda S, et al. 24.7% record efficiency HIT solar cell on thin silicon wafer. *IEEE J Photovolt*. 2014;4(1):96-99.
- Masuko K, Shigematsu M, Hashiguchi T, et al. Achievement of more than 25% conversion efficiency with crystalline silicon heterojunction solar cell. *IEEE J Photovolt*. 2014;4(6):1433-1435.
- Yoshikawa K, Kawasaki H, Yoshida W, et al. Silicon heterojunction solar cell with interdigitated back contacts for a photoconversion efficiency over 26%. *Nat Energy*. 2017;21:17032-1-17032-8.
- Green MA, Emery K, Hishikawa Y, Warta W, Dunlop ED. Solar cell efficiency tables (version 48). *Prog Photovolt*. 2016;24(7):905-913.
- Goetzberger A, Luther J, Willeke G. Solar cells: past, present, future. *Sol Energy Mater Sol Cells*. 2002;74(1-4):1-11.
- Yamaguchi M, Lee KH, Araki K, Kojima N. A review of recent progress in heterogeneous silicon tandem solar cells. *J Phys D: Appl Phys*. 2018; 51:13302-1-13302-13.
- Ahrenkiel RK. Minority-carrier lifetime in III-V semiconductors. In: Ahrenkiel RK, Lundstrom MS, eds. *Semiconductors and Semimetals*. Vol. 39, Chapter 2 Boston: Academic Press; 1993 pp. 58.
- Yamaguchi M, Yamada H, Katsumata Y, Lee KH, Araki K, Kojima N. Efficiency potential and recent activities of high-efficiency solar cells. *J Mater Res*. 2017;32(18):3445-3457.
- Yamaguchi M, Lee KH, Araki K, Kojima N, Ohshita Y. Analysis for efficiency potential of crystalline Si solar cells. *J Mater Res*. 2018;33(17): 2621-2626.
- Rau U. Reciprocity relation between photovoltaic quantum efficiency and electroluminescent emission of solar cells. *Phys Rev B*. 2007;76: 085303-1-085303-8.
- Green MA. Radiative efficiency of state-of-the-art photovoltaic cells. *Progress in Photovoltaics*. 2012;20(4):472-476.
- Yao J, Kirchartz T, Vezie MS, et al. Quantifying losses in open-circuit voltage in solution-processable solar cells. *Phys Rev Applied*. 2015; 4(1):014020-1-014020-10.
- Zhu L, Lee KH, Yamaguchi M, et al. Analysis of nonradiative recombination in quantum dot cells and materials. *Prog Photovolt*. 2019; 27(11):971-977.
- Swanson R. Approaching the 29% limit efficiency of silicon solar cells. *Proceedings of the 20th European Photovoltaic Solar Energy Conference (WIP, Munich)*. 2005:pp. 584.
- Richter A, Hermle M, Glunz SW. Reassessment of the limiting efficiency for crystalline silicon solar cells. *IEEE J Photovolt*. 2013;3(4): 1184-1191.
- Green MA. *Solar Cells*. Kensington: UNSW; 1998.
- PV education, standard solar spectra. <https://www.pveducation.org/pvcdrom/appendices/standard-solar-spectra>
- Yamaguchi M, Nagai O. Effects of impurities on gamma-irradiated silicon crystal examined by photovoltaic effect of p-n junction diode. *Jpn J Appl Phys*. 1972;11(7):1016-1023.
- Yamaguchi M, Khan A, Taylor SJ, Imaizumi M, Hisamatsu T, Matsuda S. A detailed model to improve the radiation-resistance of Si space solar cells. *IEEE Trans Elect Dev*. 1999;ED-46:2133-2138.
- Downing RG, Carter JR, Denny JH. The energy dependence of electron damage in silicon. *Proceedings of the 4th IEEE Photovoltaic Specialists Conference*. (IEEE, New York, 1962) 1962:p.A-5-1-A-5-33.
- Yamaguchi M, Khan A, Taylor SJ, et al. Deep level analysis of radiation-induced defects in Si crystals and solar cells. *J Appl Phys*. 1999;86(1):217-223.
- Khan A, Yamaguchi M, Aburaya T, Matsuda S. Evolution of defect complexes in Si single crystals with heavy fluence 10MeV proton irradiation. *J Appl Phys*. 2000;87(5):2162-2168.
- Lammert MD, Schwarz RJ. The interdigitated back-contact solar cell: a silicon solar cell for use in concentrated sunlight. *IEEE Trans Elec Dev*. 1977;ED-24:337-342.
- Swanson RM. Point contact silicon solar cells. *Proceedings of the 17th IEEE Photovoltaic Specialists Conference*, (IEEE, New York). 1984: 1294-1296.
- Snow EH, Grove AS, Fitzgerald DJ. Effects of ionizing radiation on oxidized silicon surfaces and planar devices. *Proc IEEE*. 1967;55(7): 1168-1185.
- Yamaguchi M. Fundamentals and R&D status of III-V compound solar cells and materials. *Phys Status Solidi (c)*. 2015;6:489-499.

32. Basore PA, Clugston DA. PC1D version 4 for Windows: from analysis to design. *Proceedings of the 25th IEEE Photovoltaic Specialists Conference*, (IEEE, New York) 1996:p. 377–381.
33. Clugston DA, Basore PA. 32-bit solar cell modelling on personal computers. *Proceedings of the 26th IEEE Photovoltaic Specialists Conference*, (IEEE, New York) 1997:p.207–210.
34. Masuda S, Imaizumi M, Anzawa O, et al. Radiation effects in space on solar cells developed for terrestrial use demonstrated by MDS-1. *Proceedings of the 3rd World Conference on Photovoltaic Energy Conversion*, (WCPEC, 2003) 2003:p. 642–645. ISBN 4-9901816-0-3.
35. Garboushian V, Yoon S, Turner J. Radiation hardened high efficiency silicon space solar cell. *Proceedings of the 23rd IEEE Photovoltaic Specialists Conference*, (IEEE, New York.) 1993: p. 1358–1362.
36. Carter JR Jr. Effects of electron damage on defect introduction in silicon. *J Phys Chem Solid.* 1966;27(6-7):913-918.
37. Londos CA. Defect states in electron-bombarded n-type silicon. *Phys Status Sol (a)*. 1989;113:503-510.
38. Markevich VP, Peaker AR, Lastovskii SB, Gusakov VE, Medvedeva IF, Murin LI. Formation of radiation-induced defects in Si crystals induced with electron at elevated temperatures. *Solid State Phenom.* 2010;156–158:299-304.

How to cite this article: Yamaguchi M, Lee K-H, Araki K, Kojima N, Okuno Y, Imaizumi M. Analysis for nonradiative recombination loss and radiation degradation of Si space solar cells. *Prog Photovolt Res Appl.* 2020;1–11. <https://doi.org/10.1002/pip.3346>